arXiv:physics/0211076v1 [physics.plasm-ph] 17 Nov 2002

# Nyquist Method for Wigner-Poisson Quantum Plasmas

F. Haas*
Laboratório Nacional de Computação Científica - LNCC
Av. Getúlio Vargas, 333
25651-07 Petrópolis, RJ, Brazil
G. Manfredi†
Laboratoire de Physique des Milieux Ionisés, Université Henri Poincaré,
BP 239, 54506 Vandoeuvre-les-Nancy, France
J. Goedert‡
Centro de Ciências Exatas e Tecnológicas - UNISINOS
Av. Unisinos, 950
93022-000 São Leopoldo, RS, Brazil

February 2, 2008

**Abstract**

By means of the Nyquist method, we investigate the linear stability of electrostatic waves in homogeneous equilibria of quantum plasmas described by the Wigner-Poisson system. We show that, unlike the classical Vlasov-Poisson system, the Wigner-Poisson case does not necessarily possess a Penrose functional determining its linear stability properties. The Nyquist method is then applied to a two-stream

*ferhaas@lncc.br
†giovanni.manfredi@lpmi.uhp-nancy.fr
‡goedert@exatas.unisinos.br

distribution, for which we obtain an exact, necessary and sufficient condition for linear stability, as well as to a bump-in-tail equilibrium.

*PACS numbers: 52.30.-q, 52.35.-g, 52.90.+z, 05.60.Gg*

# 1 Introduction

The topic of quantum plasmas has recently attracted considerable attention [1]-[9]. A central reason for this accrued interest derives from the importance of quantum effects in the performance of today's micro-electronic devices, for which classical transport models are not always adequate in view of the increasing miniaturization level that is now entering the submicron domain. Hence, it is desirable to achieve a good understanding of the basic properties of quantum transport models. The Wigner-Poisson system [10]-[12] is a quantum transport model that has proven to be suitable in the treatment of quantum devices like the resonant tunneling diode [1]. Moreover, it has been referred [13] to as perhaps the only *kinetic* quantum transport model amenable to detailed numerical simulation. In the present work, we address the question of the stability of small-amplitude waves, described by the Wigner-Poisson system.

A convenient tool to investigate the linear stability of systems having a dispersion relation is provided by the Nyquist method [14],[15]. Let us briefly review the basis of this approach. Let $D(\omega, k) = 0$ be the dispersion relation, where $\omega$ and $k$ are the frequency and wave-number for small-amplitude oscillations. In most practical cases, it is impossible to solve exactly the dispersion relation for $\omega$ as a function of $k$, some kind of approximation being necessary. Hence, the imaginary part of the frequency, which determines the stability properties of the system, can be obtained only in an approximate way. However, exact results can be found by splitting $D$ in its real and imaginary parts, $D(\omega, k) = D_r(\omega, k) + iD_i(\omega, k)$. Then, for fixed $k$ and real $\omega$, by varying $\omega$ from minus to plus infinity we can draw a diagram in the $D_r \times D_i$ plane. The resulting curve, known as the Nyquist diagram, determines the number of unstable modes of the system, which equals the number of times the origin is encircled by the diagram [14]. For example, using the Nyquist

method, one can show that equilibrium distributions that are monotonically decreasing functions of the energy are stable against small perturbations. Moreover, for symmetric equilibria with at most two maxima, the sign of the so-called Penrose functional [14],[15] determines the linear stability of the classical Vlasov-Poisson system.

In view of the utility of Nyquist's method for classical plasmas, it seems desirable to investigate whether it can be applied to the quantum case too. This approach is justified, since the linear stability of waves in the Wigner-Poisson system is described by a dispersion relation, and is therefore amenable to Nyquist's treatment. However, we cannot a priori expect to obtain a result as general as in the classical case. Indeed, as we shall see, the question of stability is subtler in the quantum framework, a typical example being provided by the two-stream instability [16]. For simplicity, in the present work we shall only consider homogeneous equilibria for one-dimensional electrostatic plasmas consisting of mobile electrons. An immobile ionic background guarantees overall charge neutrality.

The paper is organized as follows. In Section II, we develop the fundamentals of the Nyquist method as applied to quantum plasmas described by the Wigner-Poisson system. The stability properties of quantum plasmas are determined by the specific form of the quantum dispersion relation [17],[18]. We show that there are a rich variety of possible behaviors in quantum systems, which are not present in classical Vlasov-Poisson plasmas. In particular, in Section III, we prove that a quantum analogue of the Penrose functional cannot exist. To show this, we consider symmetric equilibria with at most two maxima. Nevertheless, the Nyquist method can still be used for Wigner-Poisson plasmas. This is explicitly shown in Section IV, where we study a two-stream equilibrium, described by a bi-Lorentzian distribution function, which is amenable to exact calculations. We find an exact criterion for stability, which reduces to the classical criterion when quantum effects becomes negligible. However, large quantum effects can destroy the instability occurring in the purely classical case. In Section IV, we also include the example of the physically relevant distribution corresponding to a bump-in-tail equilibrium. Our conclusions are given in Section V.

## 2 Quantum dispersion relations

If $f(x,v,t)$ is the Wigner quasi-distribution and $\phi$ the scalar potential, then the Wigner-Poisson system [10]-[12] reads

$$\frac{\partial f}{\partial t} + v\frac{\partial f}{\partial x} = \int dv' K(v'-v,x,t) f(v',x,t)\,, \tag{1}$$

$$\frac{\partial^2 \phi}{\partial x^2} = \frac{e}{\varepsilon_0}(\int dv\, f - n_0)\,, \tag{2}$$

where $K(v'-v,x,t)$ is a functional of the scalar potential,

$$K(v'-v,x,t) = \frac{em}{i\hbar}\int \frac{d\lambda}{2\pi\hbar}\exp\left(\frac{im(v'-v)\lambda}{\hbar}\right)\times$$
$$\times \left(\phi(x-\frac{\lambda}{2},t) - \phi(x+\frac{\lambda}{2},t)\right). \tag{3}$$

Here, $n_0$ is a background ionic density, $-e$ and $m$ are the electron charge and mass, $\hbar$ is the scaled Planck constant and $\varepsilon_0$ is the vacuum dielectric constant. We take periodic boundary conditions in space and assume that for large $|v|$, $f$ and all its velocity derivatives tend to zero. We also assume that the initial Wigner function is everywhere positive. However, the time evolution determined by Eq. (1) may force the Wigner function to assume negative values. Hence, a strict interpretation of $f$ as a true probability distribution is impossible. In spite of that, the Wigner function may be used as a useful mathematical tool to compute macroscopic quantities such as the charge density and electric current.

The linear stability of a plasma, be it classical or quantum, is determined by the dispersion relation, which is obtained after Fourier transforming in space and Laplace transforming in time. Following this procedure, we obtain [17] for a frequency $\omega$ and a wave number $k$

$$D(k,\omega) = D_r(k,\omega) + iD_i(k,\omega) = 0\,, \tag{4}$$

where the dispersion function $D(k,\omega)$ is given by

$$D_r(k,\omega) = 1 - \frac{\omega_p^2}{n_0 k^2}\int_P \frac{dv\, F(v)}{(v-\omega/k)^2 - \hbar^2 k^2/4m^2}\,, \tag{5}$$

$$D_i(k,\omega) = -\frac{\pi\, e^2}{\hbar\varepsilon_0 k^3}\left(F(\frac{\omega}{k}+\frac{\hbar\, k}{2m}) - F(\frac{\omega}{k}-\frac{\hbar\, k}{2m})\right). \tag{6}$$

In Eq. (5), $P$ stands for the principal value symbol and $F(v)$ denotes the (spatially homogeneous) equilibrium Wigner function. Also, $\omega_p = (n_0 e^2/m\varepsilon_0)^{1/2}$ is the usual plasma frequency.

The quantum formulae reduce to the classical ones as $\hbar \to 0$. In particular,

$$D_i(k,\omega) = -\frac{\pi\omega_p^2}{n_0 k^2}\left(\frac{dF}{dv}\right)_{v=\omega/k} + O(\hbar^2)\,. \tag{7}$$

Moreover, no matter what the value of $\hbar$, for $|\omega| \to \infty$ we have $D_r \to 1$ and $D_i \to 0$, as in the classical case.

The topology of the Nyquist diagram is determined by the sign of $D_r$ at the points where $D_i = 0$. As mentioned in the Introduction, the number of unstable modes equals the number of times the Nyquist curve encircles the origin. Therefore, unstable modes can only exist if $D_r < 0$ for at least one of the points where $D_i = 0$. In the classical case, the zeroes of the imaginary part of the dispersion function are determined by the points at which the distribution function has zero derivative. In the quantum case, according to Eq. (6), the decisive points are the real roots $v_0$ of

$$F(v_0 + H) = F(v_0 - H)\,. \tag{8}$$

Here and in the following,

$$v_0 = \frac{\omega}{k}\,, \quad H = \frac{\hbar\, k}{2m}\,. \tag{9}$$

The geometrical interpretation of Eq. (8) is simple: we have to find the points $v_0$ that are equidistant to any two points at which $F$ has the same value (see Fig. 1). The corresponding distance is $H$. In a sense, Eq. (8) is the finite difference version of the classical condition $dF/dv(v = v_0) = 0$. Finally, as Nyquist's diagram is obtained taking exclusively real frequencies, only the real roots of Eq. (8) are relevant.

The basic tasks we have to perform are first solving Eq. (8), obtaining all real roots $v_0$ for a given $H$, and then studying the sign of $D_r$ at each such root, taking $\omega = k\, v_0$. Using Eq. (5), we have

$$D_r(k, \omega = k v_0) = 1 - \frac{\omega_p^2}{n_0 k^2}\int_P dv\, \frac{F(v)}{(v - v_0)^2 - H^2}\,. \tag{10}$$

Now, in the Cauchy principal value sense,

$$\int_P \frac{dv}{(v-v_0)^2 - H^2} = 0\,. \tag{11}$$

Using this fact, we can rewrite the real part of the dispersion function in the more convenient way

$$D_r(k, \omega = kv_0) = 1 + \frac{\omega_p^2}{n_0 k^2} \int dv\, \frac{F(v_0 + H) - F(v)}{(v-v_0)^2 - H^2}\,. \tag{12}$$

In this form, the principal value symbol is not needed anymore, since the integrand is regular as $v$ goes to $v_0 \pm H$. Indeed, using the fact that $F(v_0 + H) = F(v_0 - H)$ from Eq. (8), we find that

$$\lim_{v \to v_0 \pm H} \frac{F(v_0 + H) - F(v)}{(v-v_0)^2 - H^2} = \mp \frac{1}{2H} \frac{dF}{dv}(v_0 \pm H) \tag{13}$$

is a finite quantity. A similar (but not identical) regularization procedure holds in the classical case too [14].

Equations (8) and (12) are the fundamental equations for Nyquist's method for one-dimensional quantum plasmas, in which only electrostatic fields are present. So far, the treatment has been completely general. Let us now consider some particular equilibria in order to analyze the consequences of Eqs. (8) and (12).

# 3 Equilibria with one or two maxima

If the equilibrium Wigner function $F(v)$ has a single maximum $v_{max}$, then the geometric meaning of $v_0$ is sufficient to show that Eq. (8) has always one, and only one, real solution $v_0$ for any value of $H$ (see Fig. 1). Depending on the shape of $F$, this solution can differ considerably from $v_{max}$ (one has $v_0 = v_{max}$ when $F$ is symmetric with respect to $v_{max}$). However, as $H$ goes to zero, and again from geometrical arguments, we can convince ourselves that $v_0$ approaches $v_{max}$. Indeed by definition $v_0$ is equidistant to the points $v'$ and $v''$ for which $F(v') = F(v'')$. The corresponding distance from $v_0$ to either $v'$ or $v''$ is $H$.

Furthermore, for $(v - v_0)^2 > H^2$ we have $F(v_0 + H) > F(v)$ and for $(v - v_0)^2 < H^2$ we have $F(v_0 + H) < F(v)$. Hence, the integrand in Eq. (12) is always positive, implying that the real part of the dispersion function is a positive quantity. Also, for $|\omega| \to \infty$ we have $D_r \to 1$ and $D_i \to 0$. Since there is only one root for Eq. (8), we deduce that the Nyquist diagram cannot encircle the origin, and therefore no unstable modes can exist for an equilibrium with a single maximum. Thus, no matter how strong quantum effects are, the conclusion is the same as for the classical case.

Let us now consider equilibria with a single minimum, $v_{min}$ (see Fig. 2). This is equivalent to consider equilibrium Wigner functions with only two maxima, as on physical grounds the equilibrium function must decay to zero as $|v| \to \infty$. Physically, such equilibria correspond to a situation where two counterstreaming electron populations (with similar temperatures) co-exist. In the classical case, the Nyquist diagram for this situation leads to the construction of the so-called Penrose functional

$$P[F] = \int dv \frac{F(v_{min}) - F(v)}{(v_{min} - v)^2}\,, \tag{14}$$

which determines the stability properties of the system. The inequality $P[F] < 0$ is a necessary and sufficient condition for instability, for appropriate wave numbers. This can be easily seen from the classical limit $H \to 0$ of Eq. (12). Classically, the points $v_0$ where $D_i = 0$ are the maxima ($\pm v_{max}$) and the minimum ($v_{min}$) of the equilibrium distribution. For $v_0 = \pm v_{max}$, the integrand in Eq. (12) is always positive, and thus cannot lead to instability. For $v_0 = v_{min}$, the real part of the dispersion function reduces to $D_r = 1 + (\omega_p^2/n_0 k^2)\ P[F]$. If the Penrose functional is positive, instability is ruled out. If it is negative, one can always choose $k$ small enough so that $D_r < 0$ and therefore some unstable modes must exist. This completes the proof of the necessary and sufficient Penrose criterion.

The natural question now is whether there exists an analogue Penrose functional for the quantum case. For simplicity, in the following we restrict our discussion to Wigner equilibria that are symmetric about $v_{min}$, the point at which $F$ attains its minimum value. By a Galilean transformation, this point can be taken as $v_{min} = 0$ without loss of generality. We first notice that, in the classical case, one only has to consider the three velocities for which

the equilibrium distribution function has zero derivative. In the quantum case, however, depending on the shape of the equilibrium Wigner function, there can be more then three roots for Eq. (8), with fixed $H$. For instance, in Fig. 2, root $v_1$ (connecting one increasing and one decreasing branch of the distribution) can be obtained from the local maximum $v_{max}$, by varying $H$ continuously from zero to a certain value. The root $v_2$ (connecting two decreasing branches of the distribution) is of a different nature, arising only for sufficiently large $H$. Indeed, it is not difficult to realize that, in the case of two maxima, there are always only three roots for Eq. (8) if $H$ is small enough, and up to five roots for larger values of $H$. Also notice that, for symmetric equilibria, the point $v = 0$ is always a root, irrespective of the value of $H$. For a given $H$, possessing one, three or five real roots depends on the details of the equilibrium. It is not difficult to prove that, in the case of a two-humped distribution, a sufficient (but not necessary) condition for having five roots to Eq. (8) is that $F(v_{min}) = 0$. This can be shown by plotting the left- and right-hand sides of Eq. (8) as a function of $v_0$, and looking at the intersections of the two curves. In general, we obtain that one can have five solutions when $F(v_{min})$ is smaller than a certain threshold. Note however that five roots only appear for sufficiently large values of $H$; for small enough $H$, there are always only three roots. In Section IV, we shall examine a bi-Lorentzian distribution possessing at most three solutions. In addition, we shall discuss another two equilibria, which possess five solutions for sufficiently large $H$.

Let us now consider the question of the existence of a quantum Penrose functional. We need to examine the sign of $D_r$ at the different solutions of Eq. (8). The root $v_0 = v_{min} = 0$ always exists and can yield either a positive or a negative value for the integral in Eq. (12), depending on the shape of the equilibrium and the value of $H$. One can actually prove that the integral can be negative only if $H < v^\star$, where $v^\star$ is the positive solution of the equation $F(0) = F(v^\star)$.

We now analyze the other roots of Eq. (8). Let $v_1$ be the root obtained from the maximum of $F$ at the right of $v = 0$ by varying continuously $H$ from zero to some particular value (see Fig. 2). Referring to Fig. 2 and to Eq. (12) (with $v_0 = v_1$), we conclude that the integrand in $D_r$ is negative for

$-v_1 - H < v < -v_1 + H$. Thus, in principle, the real part of the dispersion function can be negative. However, one could imagine that the negative contribution for $-v_1 - H < v < -v_1 + H$ is compensated by a positive contribution corresponding to $v_1 - H < v < v_1 + H$. Let us examine this possibility. Using the fact that $F$ is even, we obtain

$$\begin{aligned} \int_{-v_1-H}^{-v_1+H} dv \;\; \frac{F(v_1+H)-F(v)}{(v-v_1)^2-H^2} + \int_{v_1-H}^{v_1+H} dv \, \frac{F(v_1+H)-F(v)}{(v-v_1)^2-H^2} = \\ = \;\; 2\int_{v_1-H}^{v_1+H} dv \, \frac{(F(v_1+H)-F(v))(v^2+v_1^2-H^2)}{(v^2-(H+v_1)^2)(v^2-(H-v_1)^2)} \, . \end{aligned} \tag{15}$$

For $v_1 - H < v < v_1 + H$, we have $F(v) > F(v_1 + H)$, $v^2 > (H - v_1)^2$ and $v^2 < (H + v_1)^2$. Hence, the integrand in Eq. (15), which can give the only negative contribution for $D_r$, is negative provided

$$v^2 < H^2 - v_1^2 \, , \tag{16}$$

which is impossible in the prescribed range of velocities, as $v_1 > H$ by construction. Therefore, we always have $D_r(k, \omega = kv_1) > 0$, where $v_1$ is the (semi-classical) root for Eq. (8) obtained from the positive maximum of $F$, and the same argument holds for the symmetric root $-v_1$. This is analogous to the classical result shown above, according to which $D_r$ is positive at the two maxima of $F(v)$. Indeed, the roots $\pm v_1$ coincide with $\pm v_{max}$ when $H \to 0$.

However, this is not the end of the story for the quantum case. Indeed, for sufficiently large values of $H$, it is possible to access the roots $\pm v_2$ (connecting two decreasing branches of the distribution) shown on Fig. 2. [This is not in contradiction with the above statement that some equilibria only display three solutions to Eq. (8). Solutions of the type $v_2$ always exist, although they may correspond to *different values of* $H$ than $v_1$, so that for a fixed $H$ there are indeed only three roots]. For the roots $\pm v_2$, which are of a strictly quantum nature, we cannot anymore obtain, a priori, $D_r > 0$. For instance, for the particular choice of $v_2$ shown on Fig. 2, the region $-v_2 - H < v < -v_2 + H$ contributes a negative value to $D_r(k, \omega = kv_2)$. The same is true for the root $-v_2$. This is because, over most of the region $-v_2 - H < v < -v_2 + H$

one has $F(v_2 + H) < F(v)$ and $(v - v_2)^2 > H^2$, implying that the integral in Eq. (12) is negative. Another choice of $v_2$ may have yielded the opposite result, so that the sign of $D_r(k, \omega = kv_2)$ cannot be determined a priori. As the parameter $H$ depends on the wave number, it is always possible to choose $k$ so as to access a root of the type $\pm v_2$, for which the sign of $D_r$ is undetermined. The conclusion is that there is *no* quantum Penrose functional, since the topology of the Nyquist diagram can be changed, in an essential way, by the value of $D_r$ at the quantum roots for Eq. (8). Each specific equilibrium must be studied in detail. In the following Section, we shall illustrate the previous theory using some concrete examples.

# 4 Examples of two-stream and bump-in-tail equilibria

Let us consider a two-humped equilibrium given by

$$F(v) = \frac{n_0 \Delta}{2\pi} \left( \frac{1}{(v-a)^2 + \Delta^2} + \frac{1}{(v+a)^2 + \Delta^2} \right) , \tag{17}$$

where $\Delta$ is a measure of the dispersion of the distribution and $a$ is a parameter associated to the distance between the two possible maxima. If $a^2 < \Delta^2/3$ this bi-Lorentzian distribution degenerates into a one-humped equilibrium, which is consequently stable against linear perturbations, both in classical and quantum cases. The major advantage of dealing with Eq. (17) is that it is amenable to exact calculations, thus providing an appropriate example of the use of the Nyquist method for quantum plasmas. Moreover, it models the physically relevant situation of two counterstreaming electron populations that co-exist within the same plasma.

Inserting Eq. (17) into Eq. (8), we obtain the following solutions,

$$v_0^0 = 0 , \tag{18}$$

$$v_0^1 = \pm \left( H^2 - a^2 - \Delta^2 + 2\sqrt{a^2 + \Delta^2}\sqrt{a^2 - H^2} \right)^{1/2} , \tag{19}$$

$$v_0^2 = \pm \left( H^2 - a^2 - \Delta^2 - 2\sqrt{a^2 + \Delta^2}\sqrt{a^2 - H^2} \right)^{1/2} . \tag{20}$$

It is easy to check that the roots given in Eq. (20) are always complex, whatever the values of $H$, $a$ and $\Delta$. However, the roots (19) can be real, provided

$$a^2 > \frac{1}{3}(H^2 - \Delta^2) + \frac{2}{3}(\Delta^4 + H^2\Delta^2 + H^4)^{1/2} \,. \tag{21}$$

Thus, there can be one or three relevant roots, according to condition (21). This inequality, when satisfied, can also be seen to imply $a^2 > \Delta^2/3$, which is the same as the condition for the existence of two maxima. Hence, there can be three real roots if and only if $F$ is two-humped, which is not surprising in view of the arguments given in the preceding Section.

An equivalent and illuminating way to rewrite Eq. (21) is

$$H^2 < v_{max}^2 \,, \tag{22}$$

where $v_{max}$ denotes the (positive) point where $F$ is maximum,

$$v_{max} = (a^2 + \Delta^2)^{1/4} \left(2a - \sqrt{a^2 + \Delta^2}\right)^{1/2} \,. \tag{23}$$

Hence, $2H$ cannot exceed the distance between the two maxima of $F$. Notice that the right hand side of Eq. (23) can be real only if $a^2 > \Delta^2/3$, that is, if there are two maxima, which is again a natural result. For very large quantum effects, only the root $v_0^0 = 0$ survives.

As there is no quantum Penrose functional, it is necessary to calculate $D_r$ at all possible roots (18)-(19). We obtain

$$D_r(k, \omega = kv_0^0 = 0) = 1 + \frac{\omega_p^2}{k^2} \frac{(\Delta^2 + H^2 - a^2)}{(H^2 - a^2)^2 + 2\Delta^2(H^2 + a^2) + \Delta^4} \,, \tag{24}$$

which can be negative if and only if

$$a^2 > \Delta^2 + H^2 \,. \tag{25}$$

In addition,

$$D_r(k, \omega = \pm kv_0^1) = 1 + 16 \, \frac{\omega_p^2 \sqrt{a^2 + \Delta^2}(a^2 - H^2)a^2\delta}{k^2 U^8} \,, \tag{26}$$

where $\delta$ and $U^8$ are the positive-definite quantities

$$\begin{aligned} \delta &= \sqrt{a^2+\Delta^2}-\sqrt{a^2-H^2}\,, \qquad (27) \\ U^8 &= \left(((v_0-H)^2-a^2)^2+2\Delta^2((v_0-H)^2+a^2)+\Delta^4\right)\times \\ &\times \left(((v_0+H)^2-a^2)^2+2\Delta^2((v_0+H)^2+a^2)+\Delta^4\right). \qquad (28) \end{aligned}$$

We can show that Eq. (21) implies $a^2 > H^2$, so that $D_r$ as given by Eq. (26) is indeed always positive.

In view of Eqs. (24) and (26), we see that Eq. (25) is a necessary and sufficient condition for linear instability. That this condition is sufficient can be easily proven: suppose that we have found a wave number $k_0$ satisfying Eq. (25); then any $k < k_0$ will also satisfy it; by taking $k$ small enough, we can make the second addendum of Eq. (24) (which is negative) arbitrarily large in absolute value and therefore obtain $D_r < 0$. Note, however, that putting an equality sign in Eq. (25) and solving for $k$ does *not* provide the transition wave number between stable and unstable behavior. In order to obtain it, one has to set Eq. (24) to zero and solve for $k$.

Equation (25) means that the plasma can become unstable for sufficiently large $a$ (the two maxima are sufficiently far apart), small $\Delta$ (small dispersion) or small $H$ (small quantum effects). We also notice that, as $H$ depends on the wave number, quantum effects can suppress the instability for small wavelengths. The instability condition Eq. (25) confirms the numerical results by Suh *et al.* [19]. Here, however, we have derived an *exact* analytical criterion for quantum linear stability of a two-stream equilibrium.

On Fig. 3, we have plotted the Nyquist diagrams for the two-stream equilibrium of Eq. (17) with $a = 3$, $\Delta = 1$, $k = 0.2$ and four different values of $\hbar$ (units for which $e = \varepsilon_0 = m = n_0 = 1$ are used). We observe that stabilization of the $k = 0.2$ mode occurs somewhere between $\hbar = 25$ and $\hbar = 27$. This is in agreement with the previous formulae: indeed, with this set of parameters, it is found that $D_r(k, \omega = kv_0^0)$ changes sign for $\hbar \simeq 25.5$. Furthermore, Fig. 3 also shows a change in the topology of the Nyquist diagram. For figures (a)−(c), the diagram intersects the horizontal axis in three points [excluding the point (1,0) that corresponds to $\omega = \pm\infty$]; note that two such points coincide, because of the symmetry of the distribution. For figure (d), only one intersection survives. This change in topology corresponds to

having one or three solutions to Eq. (8), which is determined by Eq. (21). The transition is found to occur for $\hbar \simeq 30$, which is in agreement with the diagrams of Fig. 3.

Finally, we point out that large quantum effects are not necessarily stabilizing. For the two-stream equilibrium of Eq. (17), with $a = 3$ and $\Delta = 1$, the wave number $k = 0.287$ is classically stable. However, increasing $\hbar$, one finds that $D_r(k, \omega = kv_0^0)$ becomes negative on an interval approximately given by $7 < \hbar < 11.8$. This can be easily verified by plotting Eq. (24) as a function of $\hbar$ or by direct substitution of the above values. However, this destabilizing effect occurs for rather limited ranges of $\hbar$ and $k$. For example, wave numbers $k < 0.28$ are classically unstable and are stabilized for large enough $\hbar$ (as in our previous example with $k = 0.2$); on the other hand, wave numbers $k > 0.29$ are classically stable and remain stable for any value of $\hbar$. Only wave numbers very close to the value $k = 0.287$ display the unusual behavior described above. For this reason, we can still conclude that the most likely outcome of quantum effects is stabilization.

We now show that we can explicitly write a distribution function for which there can exist five real roots for Eq. (8). Consider the two-humped equilibrium

$$F(v) = \frac{2n_0}{\sqrt{\pi}a^3} v^2 \exp(-v^2/a^2)\,, \tag{29}$$

where $a$ is a parameter related to the equilibrium temperature. As $F(0) = 0$, we should expect that Eq. (8) possesses five real roots for some (large enough) $H$. We now give an explicit proof of this fact for the above equilibrium. The solutions to Eq. (8) are obtained in this case from the equation

$$\tanh\left(\frac{2Hv}{a^2}\right) = G(v; H)\,, \tag{30}$$

where we have defined

$$G(v; H) = \frac{2Hv}{v^2 + H^2}\,. \tag{31}$$

Apart from the obvious root $v = 0$, we can have two or four additional real roots. By plotting the left- and right-hand side of Eq. (30) as a function of $v$ (see Fig. 4), we can show that there will be a total of five real roots if and

only if

$$\frac{dG}{dv}(v=0) < \frac{d}{dv}\tanh\left(\frac{2Hv}{a^2}\right)(v=0)\,. \tag{32}$$

This implies that there can be five real roots provided $H > a$, that is, for sufficiently large quantum effects. Otherwise, only three (semi-classical) solutions are possible.

In the remaining part of this Section, we address the question of the quantum linear stability of an equilibrium characterized by a large central distribution of electrons with in addition a small bump in the tail. This is a standard problem in plasma physics, with the small perturbation to the central distribution representing a beam injected in the plasma. Here, we consider the quantum aspects of the problem, by using Nyquist diagrams. The so-called bump-in-tail equilibrium has a single minimum, but, as there is no quantum Penrose functional, we are lead to compute the real part of the dispersion function at all critical points (zeroes of the imaginary part of the dispersion function). Nevertheless, the Nyquist technique is less expensive than, for instance, direct calculation of the dispersion relation, since it requires the value of $D_r$ at a few points only.

To model the bump-in-tail equilibrium, we use the following distribution (see Fig. 5)

$$F = \frac{2n_0}{3\pi\, a}\frac{[1-\sqrt{2}(v/a)]^2}{[1+(v/a)^2]^2}\,, \tag{33}$$

where $a > 0$ is a reference velocity that can be scaled to unity without loss of generality. Henceforth, we set $a = 1$. The distribution of Eq. (33) is a particular case of a one-parameter family of bump-in-tail equilibria whose classical linear stability properties have been recently studied via Nyquist diagrams [20]. In the quantum case, there is no Penrose functional and the analysis is more involved.

Inserting Eq. (33) into the determining equation Eq. (8), we obtain the following equation for $v_0$

$$\frac{1-\sqrt{2}(v_0+H)}{1+(v_0+H)^2} = \pm\frac{1-\sqrt{2}(v_0-H)}{1+(v_0-H)^2}\,. \tag{34}$$

The plus sign yields the second-degree equation : $v_0^2 - \sqrt{2}v_0 - H^2 = 0$, with

solutions

$$v_{\pm}(H) = \frac{1}{2}\left(\sqrt{2} \pm \sqrt{6+4H^2}\right) . \tag{35}$$

Note that, in the limit $H \to 0$, these solutions correspond to the two maxima of the equilibrium distribution. Taking the minus sign in Eq. (34) yields the third-degree equation

$$\sqrt{2}v_0^3 - v_0^2 + \sqrt{2}(1-H^2)v_0 - (1+H^2) = 0 . \tag{36}$$

It is easy to prove that Eq. (36) has one real solution for $H < 3$ and three real solutions for $H \geq 3$. Furthermore, the largest of such solutions is always positive, and coincides with the minimum of the equilibrium distribution when $H = 0$ : we shall call this solution $v_m(H)$. The other two solutions (which are real only when $H \geq 3$) have no classical counterpart, and will be called $v_{q1}(H)$ and $v_{q2}(H)$. A graph of all the roots of Eq. (34) as a function of $H$ is provided on Fig. 6. Again, the existence of five real roots for some values of $H$ is a consequence of the fact that $F(v_{min}) = 0$.

As further calculations are rather cumbersome, we only report here the most relevant results (mostly obtained using the mathematical package *MAPLE*). For $H \geq 3$, we have obtained numerically, using Eq. (12), that $D_r(k, \omega = kv_{q1}) > 0$ and $D_r(k, \omega = kv_{q2}) > 0$. At least for this particular example, this can be shown to imply that the purely quantum solutions are irrelevant to the linear stability properties of the equilibrium. Moreover, we have found numerically that $D_r[k, \omega = kv_-(H)] > 0$. After an involved analysis to determine the ordering of all the solutions for Eq. (8), the conclusion is that the unstable modes satisfy

$$D_r[k, \omega = kv_m(H)] < 0 , \quad D_r[k, \omega = kv_+(H)] > 0 . \tag{37}$$

This holds whatever the value of $H$. Remembering the dependence of $H$ on the wave-number and taking into account the explicit forms of $v_m(H)$ and $v_+(H)$, it appears that the pair of conditions (37) are very complicated expressions of $k$ and $\hbar$. However, using appropriated units in which $n_0 = \omega_p = m = 1$, we were able to solve Eq. (37) numerically for a few values of $\hbar$ (measured in units of $ma^2/\omega_p$). For $\hbar = 0$, we found that the unstable modes satisfy $0.18 < k < 0.82$, where $k$ is measured in units of $\omega_p/a$. This

is the classical condition for linear instability. For $\hbar = 10$, the instability range is given by $0.20 < k < 0.36$. We see that the total band of instability becomes smaller for a non-zero Planck's constant. Further increasing $\hbar$, taking $\hbar = 100$, we found that the unstable linear waves must satisfy $0.15 < k < 0.17$. For even larger quantum effects, there is virtually a suppression of all unstable modes. This is again in agreement with the numerical results of Suh *et al.* [19], where large quantum effects were shown to stabilize all classically unstable modes for a two-stream equilibrium.

# 5 Conclusion

In this paper, we have discussed the Nyquist method for the study of the linear stability of spatially homogeneous quantum plasmas described by the Wigner-Poisson system. For classical Vlasov-Poisson plasmas, this method provides a simple way to analyze the stability properties. Furthermore, for the special case of two-stream equilibria, one can construct a simple functional (known as Penrose functional), whose sign determines whether unstable modes exist.

The main conclusion of the present work is that the stability analysis of quantum plasmas is generally subtler than in the classical case. In particular, we have shown that no simple analogue of the Penrose functional can be constructed in order to determine the stability properties of a two-humped equilibrium. Hence, a detailed analysis is necessary for each particular case, with generic and universal conclusions being more difficult to obtain. However, we were able to prove that one-humped equilibria (i.e., with a distribution that is a monotonically decreasing function of the energy) are always stable: this is the same result as for classical plasmas.

The main mathematical reason for the subtler behavior of quantum plasmas is that the wave number now enters the real part of the dispersion function through the parameter $H = \hbar k/2m$. This can change the topology of the Nyquist diagram, not only by varying $\hbar$, but also by varying the wave number at fixed $\hbar$. Physically, this means that new unstable modes can arise by resonant interaction between the quantum velocity $H$ and some other typical plasma velocity. Indeed, such purely quantum unstable modes have

been observed [16] for the special case of two-stream equilibrium

$$F(v) = \frac{n_0}{2}\delta(v-a) + \frac{n_0}{2}\delta(v+a) \ , \tag{38}$$

where $\delta$ is the Dirac delta function and $\pm a$ the velocities of each stream. This equilibrium can be amenable to exact calculation [16].

Even when general or exact results cannot be obtained, the Nyquist technique can be successfully used for the study of particular equilibria, as was shown in Section IV. The bi-Lorentzian equilibrium treated in that Section has shown that large quantum effects generally contribute to stabilize perturbations [19]. This is not always the case, however, and we have produced an explicit example of a wave number that is classically stable and becomes unstable for finite $\hbar$. Moreover, the Nyquist method has enabled us to derive an exact stability criterion for such a bi-Lorentzian equilibrium. The Nyquist technique was also applied to a classically unstable bump-in-tail equilibrium. Again, large quantum effects were shown to reduce the range of unstable wave numbers.

**Acknowledgments**
We are grateful to P. Bertrand for valuable comments and suggestions. One of us (F. H.) thanks the Laboratoire de Physique des Milieux Ionisés for hospitality while part of this work was carried out and the Brazilian agency Conselho Nacional de Desenvolvimento Científico e Tecnólogico (CNPq) for financial support.

# References

[1] N. C. Kluksdahl, A. M. Kriman, D. K. Ferry and C. Ringhofer, Phys. Rev. B **39**, 7720 (1989).

[2] F. Cornu, Phys. Rev. E **58**, 5293 (1998).

[3] B. Shokri and A. A. Rukhadze, Phys. Plasmas **6**, 3450 (1999); Phys. Plasmas **6**, 4467 (1999).

[4] G. Manfredi and M. R. Feix, Phys. Rev. E **53**, 6460 (1996).

[5] S. Mola, G. Manfredi and M. R. Feix, J. Plasma Phys. **50**, 145 (1993).

[6] J. H. Luscombe, A. M. Bouchard and M. Luban, Phys. Rev. B **46**, 10262 (1992).

[7] N. Maafa, Physica Scripta **48**, 351 (1993).

[8] C. L. Gardner, SIAM J. Appl. Math. **54**, 409 (1994).

[9] M. G. Ancona and G. J. Iafrate, Phys. Rev. B **39**, 9536 (1989).

[10] E. P. Wigner, Phys. Rev. **40**, 749 (1932).

[11] J. E. Moyal, Proc. Cambridge Phil. Soc. **45**, 99 (1949).

[12] V. I. Tatarski, Sov. Phys. Usp. **26**, 311 (1983).

[13] P. A. Markowich, C. Ringhofer and C. Schmeiser, *Semiconductor Equations* (Springer-Verlag, New York, 1990).

[14] N.A. Krall and A.W. Trivelpiece, *Principles of Plasma Physics* (McGraw-Hill, New York, 1973).

[15] R. Penrose, Phys. Fluids **3**, 258 (1960).

[16] F. Haas, G. Manfredi and M. R. Feix, Phys. Rev. E **62**, 2763 (2000).

[17] J. E. Drummond, *Plasma Physics* (McGraw-Hill, New York, 1961).

[18] Yu L. Klimontovich and V. P. Silin, Zh. Eksp. Teor. Fiz. **23**, 151 (1952).

[19] N. Suh, M. R. Feix and P. Bertrand, J. Comput. Phys. **94**, 403 (1991).

[20] D. del-Castillo-Negrete, Phys. Plasmas **5**, 3886 (1998).

Figure 1: Graphical representation of the geometric meaning of $v_0$ [solution of Eq. (8)] for a one-humped distribution function. The distance between $v_0$ and both $v'$ and $v''$ is equal to $H$. The Wigner function is represented on the vertical axis and the velocities on the horizontal axis.

Figure 2: Semi-classical ($v_0 = \pm v_1$, solid horizontal lines) and purely quantum ($v_0 = \pm v_2$, dashed horizontal line) solutions of Eq. (8) for a symmetrical two-stream equilibrium. Also note that $v_0 = 0$ (dotted line) is always a solution. Units are conveniently rescaled.

Figure 3: Nyquist diagrams for the two-stream equilibrium of Eq. (17) with $a = 3$, $\Delta = 1$, $k = 0.2$ and $\hbar = 0.001$ (a), 25 (b), 27 (c) and 40 (d) (units for which $e = \varepsilon_0 = m = n_0 = 1$ are used). Diagrams (c) and (d) indicate that quantum effects have suppressed the instability.

Figure 4: Plot of the left-hand side (solid line) and right-hand side (dashed line) of Eq. (30) as a function of $v$, for $a = 1$ and $H = 0.7$ (a) and $H = 1.2$ (b). The inset is a zoom of the region $0.9 < v < 1.4$ for case (b), showing in detail the extra solutions arising for $H > a$.

Figure 5: Velocity distribution corresponding to the bump-in-tail equilibrium of Eq. (33) for $a = n_0 = 1$.

Figure 6: Plot of the roots $v_0$ of Eq. (34) as a function of $H$. The dashed lines represent the roots $v_\pm$ in Eq. (35); the solid lines represent solutions of the cubic equation (36).

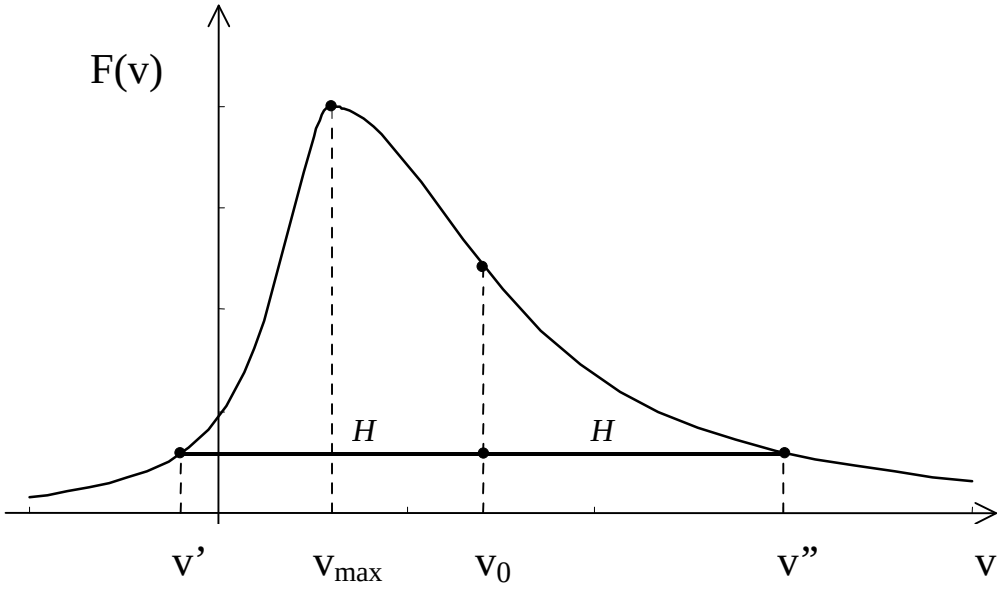


Fig. 1, Haas, PRE

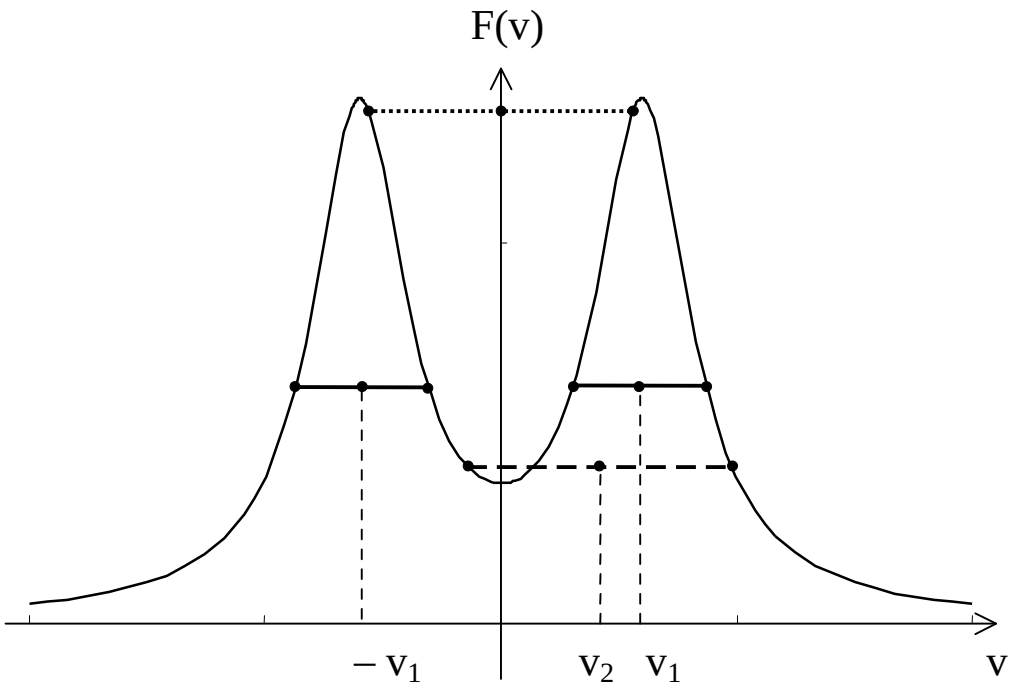


Fig. 2, Haas, PRE

Fig. 3, Haas, PRE

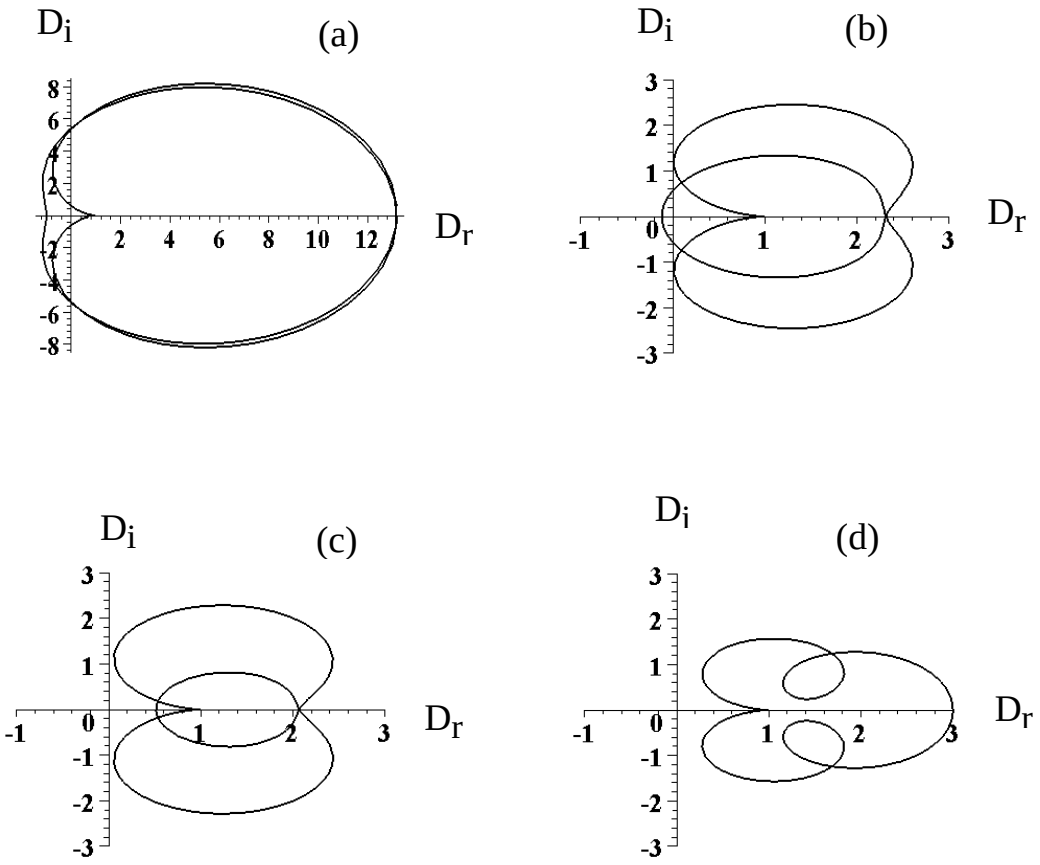

Figure 4, Haas, PRE

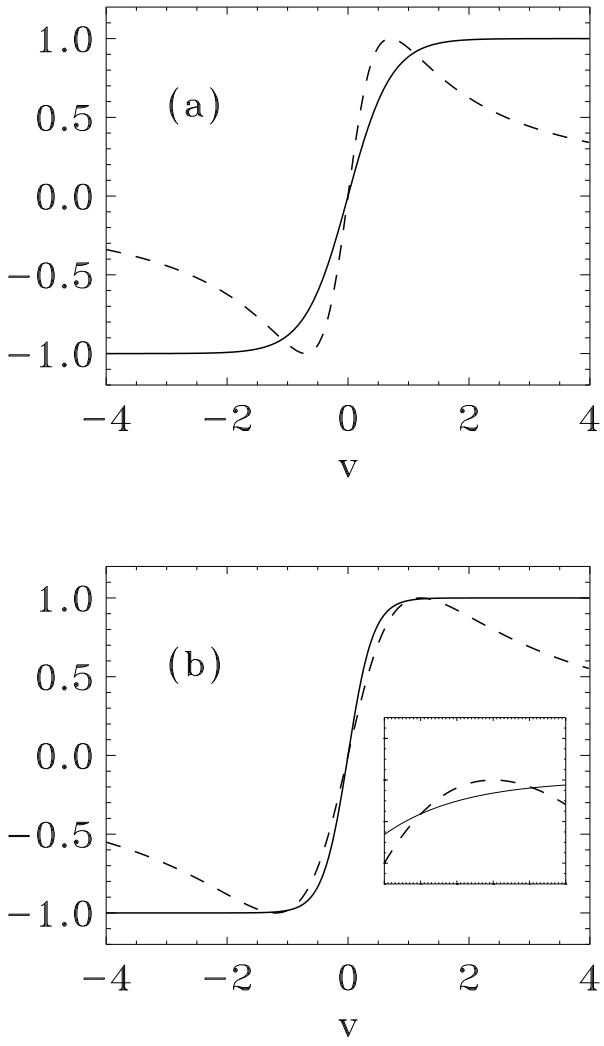

Figure 5, Haas, PRE

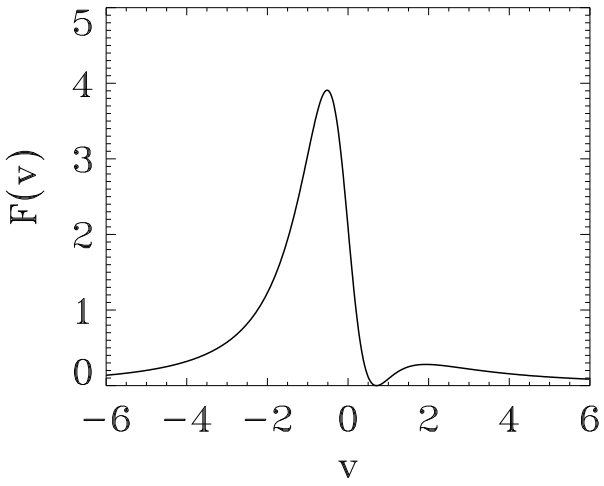

Figure 6, Haas, PRE